This article was downloaded by: [Memorial University of Newfoundland]
On: 05 August 2013, At: 13:47
Publisher: Taylor & Francis
Informa Ltd Registered in England and Wales Registered Number: 1072954 Registered office: Mortimer House, 37-41 Mortimer Street, London W1T 3JH, UK

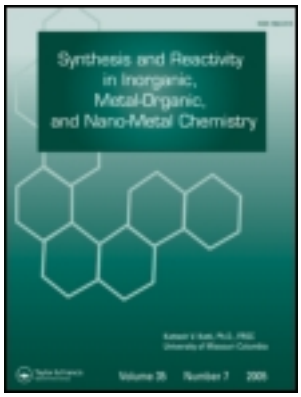

Synthesis and Reactivity in Inorganic, Metal-Organic, and Nano-Metal Chemistry
Publication details, including instructions for authors and subscription information:
http://www.tandfonline.com/loi/lsrt20

Synthesis and Characterization of the Transition Metal Complexes: Their Alcohol Oxidation and Electrochemical Properties

Mehmet Tümer [a]

[a] University of Kahramanmaraş Sütçü Imam, Faculty of Science and Arts, Department of Chemistry, Kahramanmaraş, Turkey

Published online: 19 Feb 2011.

To cite this article: Mehmet Tmer (2011) Synthesis and Characterization of the Transition Metal Complexes: Their Alcohol Oxidation and Electrochemical Properties, Synthesis and Reactivity in Inorganic, Metal-Organic, and Nano-Metal Chemistry, 41:2, 211-223

To link to this article: http://dx.doi.org/10.1080/15533174.2010.538288

PLEASE SCROLL DOWN FOR ARTICLE

Taylor & Francis makes every effort to ensure the accuracy of all the information (the "Content") contained in the publications on our platform. However, Taylor & Francis, our agents, and our licensors make no representations or warranties whatsoever as to the accuracy, completeness, or suitability for any purpose of the Content. Any opinions and views expressed in this publication are the opinions and views of the authors, and are not the views of or endorsed by Taylor & Francis. The accuracy of the Content should not be relied upon and should be independently verified with primary sources of information. Taylor and Francis shall not be liable for any losses, actions, claims, proceedings, demands, costs, expenses, damages, and other liabilities whatsoever or howsoever caused arising directly or indirectly in connection with, in relation to or arising out of the use of the Content.

This article may be used for research, teaching, and private study purposes. Any substantial or systematic reproduction, redistribution, reselling, loan, sub-licensing, systematic supply, or distribution in any form to anyone is expressly forbidden. Terms & Conditions of access and use can be found at http://www.tandfonline.com/page/terms-and-conditions

Synthesis and Reactivity in Inorganic, Metal-Organic, and Nano-Metal Chemistry, 41:211–223, 2011
Copyright © Taylor & Francis Group, LLC
ISSN: 1553-3174 print / 1553-3182 online
DOI: 10.1080/15533174.2010.538288

Taylor & Francis
Taylor & Francis Group

Synthesis and Characterization of the Transition Metal Complexes: Their Alcohol Oxidation and Electrochemical Properties

Mehmet Tümer

University of Kahramanmaraş Sütçü Imam, Faculty of Science and Arts, Department of Chemistry, Kahramanmaraş, Turkey

Downloaded by [Memorial University of Newfoundland] at 13:47 05 August 2013

Five Schiff base ligands, HA^1, HA^2, H_2L^1-H_2L^3, and their Co(II), Mn(III) and Ru(III) complexes, have been synthesized and characterized by analytical, spectroscopic, conductance, magnetic moment, and electrochemical studies. The oxidation of benzylic alcohols to the corresponding carbonyl compounds is described. In the case of some primary benzyl alcohols, high conversions were obtained. Secondary benzyl alcohol (2-hydroxy–1,2-diphenylethanone derivatives) were selectively transformed to the corresponding ketone with satisfactory conversions. The electrochemical properties of all complexes have been recorded in the different scan rates and solvents. The electrochemical properties of the complexes change with scan rates.

Keywords alcohol oxidation, electrochemical, Schiff base

INTRODUCTION

Schiff base ligands are able to coordinate metals through imine nitrogen and another group, usually linked to the aldehyde. Modern chemists still prepare Schiff bases, and nowadays active and well-designed Schiff base ligands are considered as privileged ligands. The coordination chemistry of manganese with a diverse range of ligands remains an area of considerable interest. This is not only because of the relevance that a number of model manganese complexes have to biological systems,[1] but also due to the fascinating cluster compounds, which exhibit unusual magnetic properties, and the elegant supramolecular arrays that have been discovered.[2] In addition to the interest from this inorganic standpoint, there is also considerable interest in the application of manganese complexes in organic synthesis due to their potent catalytic properties, particularly in the asymmetric epoxidation of certain olefins.[3]

The oxidation of alcohols into aldehydes and ketones is a ubiquitous transformation in organic chemistry, and numerous oxidizing agents are available to affect this key reaction.[4] In most instances, these reagents are required in stoichiometric amounts and are usually toxic, or hazardous, or both. Moreover, purification of the reaction products is often demanding and laborious. Despite the industrial importance of this process and the evergrowing environmental concerns, surprisingly few efficient catalytic oxidations of alcohols have been described.[5] The scarcity of alcohol oxidation processes that simply use oxygen or air as the ultimate stoichiometric oxidant is particularly notable.[6]

The preparation of a new ligand was perhaps the most important step in the development of metal complexes that exhibit unique properties and novel reactivity since the electron donor and electron acceptor properties of the ligand, structural functional groups, and the position of the ligand in the coordination sphere, together with the reactivity of coordination compounds, may be the factor for different studies.[7,8] Schiff bases were important class of ligands; such ligands and their metal complexes had a variety of applications including biological, clinical, analytical, and industrial, in addition to their important roles in catalysis and organic synthesis.[9–15]

In this study, the author reports the synthesis, characterization, alcohol oxidation, and electrochemical properties of the Schiff base ligands and their Co(II), Mn(III), and Ru(III) metal complexes.

EXPERIMENTAL

Materials

The metal salts $CoCl_2.6H_2O$, $Mn(AcO)_3.2H_2O$, $RuCl_3.H_2O$, and other chemicals H_2O_2, benzoylhydroperoxide, organic solvents were purchased from commercial sources and used as received, unless noted otherwise. The organic compounds *o*-vanilline, *o*-toluidine, *p*-toluidine, 1,4-di-aminobenzene, 3,5-di-aminobenzoic acid, and 1,5-di-aminonaphtalene were purchased from Fluka.

Received 21 December 2009; accepted 21 July 2010.
Address correspondence to Mehmet Tümer, University of Kahramanmaraş Sütçü Imam, Faculty of Science and Arts, Department of Chemistry, 46100, Kahramanmaraş, Turkey. E-mail: mtumer@ksu.edu.tr

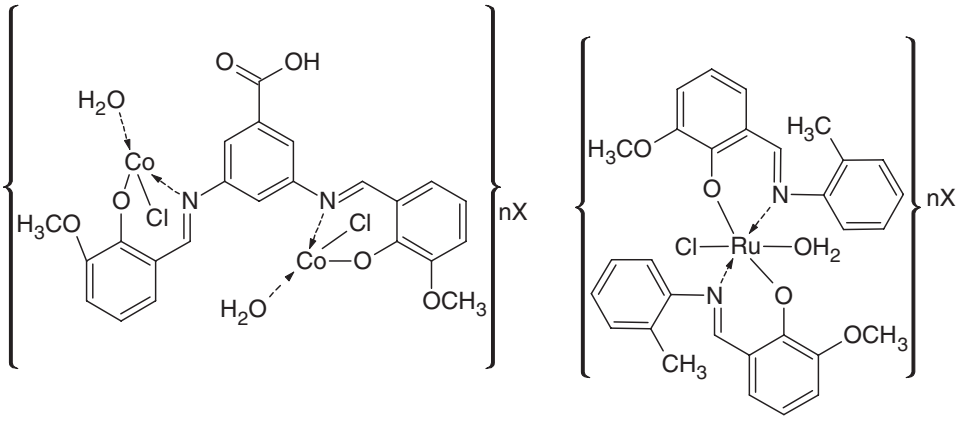

FIG. 1. Proposed structures of some synthesized metal complexes.

Downloaded by [Memorial University of Newfoundland] at 13:47 05 August 2013

Physical Measurements

Elemental analyses (C, H, N) were performed using a LECO CHNS 932 elemental analyzer. FT-IR spectra were obtained using KBr discs (4000–400 cm^{-1}) on a Shimadzu 8300 FT-IR spectrophotometer. The electronic spectra in the 200–1100 nm range were obtained on a Shimadzu UV-160 A spectrophotometer. Magnetic measurements were carried out by the Gouy method using $Hg[Co(SCN)_4]$ as calibrant. Mass spectra of the ligands were recorded on a LC/MS APCI AGILENT 1100 MSD spectrophotometer. ^{1}H-NMR spectra were recorded on a Varian XL-300 instrument. TMS was used as internal standard and deuteriated DMSO-d_6 as solvent. The metal and chloride contents of the complexes were determined as gravimetrically according to the known procedure.[16] The thermal analyses studies of the complexes were performed on a Perkin Elmer Pyris Diamond DTA/TG Thermal System under nitrogen atmosphere at a heating rate of 10°C/min. Thermal analyses studies have been done in the range 298–1273 K.

Cyclic voltammograms were recorded on an Iviumstat Electrochemical workstation equipped with a low current module (BAS PA–1) recorder. The electrochemical cell was equipped with a BAS glassy carbon working electrode (area 4,6 mm^2), a platinum coil auxiliary electrode, and a Ag/Ag^+ (0.03 M $AgNO_3$) reference electrode filled with tetrabutylammonium tetrafluoroborat (0.1 M) in DMF solvent and adjusted to 0.00 V vs SCE. Cyclic voltammetric measurements were made at room temperature in an undivided cell (BAS model C–3 cell stand) with a platinum counter electrode and an Ag/Ag^+ (0.03 M $AgNO_3$) reference electrode (BAS). All potentials are reported with respect to Ag/Ag^+ (0.03 M $AgNO_3$). The solutions were deoxygenated by passing dry nitrogen through the solution for 30 min prior to the experiments, and during the experiments, the flow was maintained over the solution. Digital simulations were performed using DigiSim 3.0 for windows (BAS, Inc.). Experimental cyclic voltammograms used for the fitting process had the background subtracted and were corrected electronically for ohmic drop.

Preperation of the Ligands

All ligands were prepared by a similar method. Solutions of *o*-vanilline (1 mmol for *o*-toluidine and *p*-toluidine; 2 mmol for 1,4-di-aminobenzene, 3,5-di-aminobenzoicacid, and 1,5-di-aminonaphtalene in 20 cm^3 EtOH) and amine derivatives (1 mmol, in 20 cm^3 EtOH) were mixed together and refluxed for about one hour in a water bath. The precipitated product was filtered and washed with cold EtOH (Figure 1). The ligands were recrystallized from hexane/EtOH (1:3 by vol) and dried in the vacuum dessiccator over P_2O_5. The purity was checked by elemental analyses and t.l.c. studies.

HA^1: ^{1}H-nmr: (DMSO-d_6 as solvent, δ in ppm): 11.05 (s, OH, H), 8.70 (s, CH=N), 6.45–7.50 (m, Ar-H, 7H), 3.75 (s, OCH_3, 3H), 2.10 (s, CH_3, 3H). Mass spectrum (LC/MS APCI): m/z 242 $[M+1]^+$ (100%), 243 $[M+2]^{+2}$ (16.9%), 227 $[C_{14}H_{13}NO_2]^{+\cdot}$ (4.2%), 167 $[C_8H_7O_4]^{+\cdot}$ (2.4%), 108 $[C_7H_{10}N]^+$ (6.3%).

HA^2: ^{1}H-nmr: (DMSO-d_6 as solvent, δ in ppm): 11.04 (s, OH, H), 8.65 (s, CH=N), 6.43–7.50 (m, Ar-H, 7H), 3.78 (s, OCH_3, 3H), 2.06 (s, CH_3, 3H). Mass spectrum (LC/MS APCI): m/z 242 $[M+1]^+$ (100%), 243 $[M+2]^{+2}$ (16.9%), 227 $[C_{14}H_{13}NO_2]^{+\cdot}$ (4.2%), 167 $[C_8H_7O_4]^{+\cdot}$ (2.4%), 108 $[C_7H_{10}N]^+$ (6.3%).

H_2L^1: ^{1}H-nmr: (DMSO-d_6 as solvent, δ in ppm): 13.09 (s, OH, 2H), 9.06 (s, CH=N, 2H), 6.95–8.15 (m, Ar-H, 10H), 3.87 (s, OCH_3, 6H). Mass spectrum (LC/MS APCI): m/z 391 $[M+1]^+$ (10%), 301 $[C_{21}H_{20}N_2+ 1]^{+2}$ (21%), 201 $[C_{13}H_{18}N_2]^{+1}$ (19.6%), 167 $[C_{11}H_7N_2]^{+3}$ (100%).

H_2L^2: ^{1}H-nmr: (DMSO-d_6 as solvent, δ in ppm): 13.21 (s, OH, 2H), 9.03 (s, CH=N, 2H), 6.68v7.55 (m, Ar-H, 12H), 3.85 (s, OCH_3, 6H). Mass spectrum (LC/MS APCI): m/z 427 $[M+1]^+$ (57.1%), 293 $[C_{18}H_{17}N_2O_2]^+$ (100%), 276 $[C_{18}H_{14}NO_2]^{+\cdot}$ (5.2%), 79 $[C_5H_3O]^+$ (38.1

H_2L^3: ^{1}H-nmr: (DMSO-d_6 as solvent, δ in ppm): 11.17 (s, COOH, 1H), 10.27 (s, OH, 2H), 9.12 (s, CH=N, 2H), 6.76–7.87 (m, Ar-H, 6H), 3.80 (s, OCH_3, 6H). Mass spectrum (LC/MS APCI): m/z 421 $[M+1]^+$ (10%), 311 $[C_{17}H_{15}N_2O_4]^{+\cdot}$ (34.1%), 312 $[C_{17}H_{16}N_2O_4]^{+2\cdot}$ (6.6%), 287 $[C_{15}H_{15}N_2O_4]^+$ (100%), 288 $[C_{15}H_{16}N_2O_4]^{+2}$ (17.0%), 289 $[C_{15}H_{17}N_2O_4]^{+3}$ (3.0%).

Downloaded by [Memorial University of Newfoundland] at 13:47 05 August 2013

Preparation of the Complexes

The complexes were prepared by similar methods. A solution of the metal salt (1 mmol for HA^1, HA^2; 2 mmol for H_2L^1-H_2L^3) in absolute EtOH (25 cm^3) was added to a solution of the ligands (2 mmol for HA^1, HA^2; 1 mmol for H_2L^1, H_2L^2 and H_2L^3) in absolute EtOH (20 cm^3) and the mixture was boiled under reflux for 6–7 h. At the end of the reaction, determined by t.l.c., the precipitate was filtered off, washed with distilled water, and then EtOH, and dried in vacuo.

Catalytic Oxidation

Catalytic oxidation of primary alcohols to corresponding aldehyde and secondary alcohol to ketone by Co(II), Mn(III) and Ru(III) complexes were studied in the presence of H_2O_2 and benzoylperoxide as cooxidant. A typical reaction using the complex as a catalyst and four benzyl alcohol derivatives, three 2-hydroxy-1,2-diphenylethanone derivatives, cyclooctanol and cyclohexanol as substrates at 1:100 molar ratio is described as follows. A solution of the complexes (0.01 mmol) in the CH_2Cl_2 (20 cm^3) was added to the solution of substrate (1 mmol) and H_2O_2 or benzoylperoxide (3 mmol). The solution mixture was refluxed for 3 h and the solvent was then evaporated from the mother liquor under reduced pressure. The solid residue was then extracted with pethroleum ether (at the room temperature or in the 60–80°C temperature range) (20 cm^3), and the ether extracts were evaporated to give corresponding aldehydes/ketones which were then quantified as 2,4-dinitrophenylhydrazone derivative.[16]

RESULTS AND DISCUSSION

In this study, I synthesized the five Schiff base ligands from the reactions between the *o*-vanilline and various amine derivatives in the ethanolic media. Analytical data are given in Table 1. The synthesized ligands are 2-methoxy-6-{(*E*)-[(4-methylphenyl)imino]methyl} phenol (HA^1), 2-methoxy-6-{(*E*)-[(2-methylphenyl)imino] methyl}phenol (HA^2), 2-{(*E*)-[(4-{[(1*E*)-(2-hydroxy-3-methoxyphenyl) methylene] amino } phenyl)imino]methyl}-6-methoxyphenol (H_2L^1), 2-{(*E*)-[(4-{[(1*E*)-(2-hydroxy-3-methoxyphenyl)methylene]amino}-1-naphthyl)imino]methyl}}-6-methox-yphenol (H_2L^2), 3-{[(1*E*)-(2-hydroxy-3-methoxyphenyl)methylene]amino}-5-{[(1*E*)-(2-hydroxy-3-methylphenyl)methylene]amino}benzoic acid (H_2L^3). If the Schiff bases are insoluble in hexane or cyclohexane, they can be purified by stirring the crude reaction mixture in these solvents, sometimes adding a small portion of a more polar solvent (Et_2O, CH_2Cl_2), in order to eliminate impurities. In general, Schiff bases are stable solids and can be stored without precautions. The ligands are more soluble in polar organic solvents as EtOH, MeOH, $CHCl_3$, DMSO, but they are partially soluble in apolar organic solvents, such as, hexane, heptane, toluene, etc. As the ligand H_2L^3 contains the COOH group on the phenylene ring, its solution is slightly acidic. The author prepared the Co(II), Mn(III), and Ru(III) complexes from these ligands, then synthesized the Ru(III) complexes according to the Co(II) and Mn(III) complexes as the low solubility of the $RuCl_3.H_2O$ in the EtOH. The ligands HA^1 and HA^2 occur the mononuclear metal complexes, whereas the complexes of the ligands H_2L^1-H_2L^3 have binuclear nature. For all complexes of the ligands, the Co(II) complexes are the most soluble while the Ru(III) are the least. The proposed structures of the some of the synthesized metal complexes are given in Figure 1.

The infrared spectral data of all compounds are given in Table 2. In the spectra of the ligands, the broad bands in the range 3420–3336 cm^{-1} can be attributed to the ν(OH) vibrations. In the complexes, this band disappear and this situation confirm that the oxygen atom of the (OH) group coordinates to the metal ions. In the spectra of the ligands, the ν(CH=N) vibrations of the azomethine groups are shown in the range 1635–1602 cm^{-1}. In the complexes, these vibrations shifted to the lower or higher regions and can be attributed to the complexation of the metal ions and nitrogen atom of the azomethine group. In the IR spectra of the complexes of the ligand H_2L^3, the COOH groups remained free as evidenced by the appearance of infrared bands in the region 1710–1725 cm^{-1}. The very slight blue-shifting from the free ligand value may be due to the combined effect of the rearrangement of the ligand structure, stereospecific interaction with the coordinated metal ion, and the presence of coordinated water in some cases. The presence of coordinated acetate group in the $[Mn(L^3)AcO(H_2O)]H_2O$ complex is confirmed by the appearance of bands at 1650 and 1360 cm^{-1}.[17] Furthermore, the presence of broad bands around 3540–3330 cm^{-1} in some of the complexes due to ν(OH) indicates presence of water molecules. Complexes show broad bands in the region 3340–3330 cm^{-1} along with the appearance of bands at 985–940 cm^{-1} (wagging modes of water) indicating coordinated water molecules.[17]

The electronic spectra of the ligands and their complexes were recorded in EtOH solvent in the region of 200–1100 nm. The spectral data are listed in Table 2. The uv spectra of the complexes $[Co(A^1)].2H_2O$, $[Mn_2(L^3)(AcO)_4(H_2O)_4].2H_2O$, $[Ru(L^1)_2Cl(H_2O)].2H_2O$ are shown in Figure 2. In the spectra of the ligands, the bands in the range 460–346 nm may be assigned to the n-π* transitions. The observed bands in the ranges 343–321 and 317–275 nm can be attributed to the π -π* and π -δ* transitions, respectively. The complexes exhibiting multiple absorptions in the UV–visible region. In the visible region, the Co(II) complexes show the d-d transitions in the range 731–617 nm. Moreover, the bands in the range 457–377 nm can be assigned to the d_π(Co)→ π*(ligand) metal to ligand charge transfer transitions. In Figure 2, the d-d and MLCT transitions of the complex $[Co(A^1)].2H_2O$ are shown. The electronic spectrum of the complex $[Mn_2(L^3)(AcO)_4(H_2O)_4].2H_2O$ in EtOH is shown in Figure 2. The absorption bands appearing in the energy region higher than ~400 nm are thought to be associated mainly with the ligand transition. In the visible and near-IR region, the spectra of the complexes exhibit one absorption bands

TABLE 1
Analytical and physical data for the Schiff base ligands and their metal complexes

Compound	Color	Yield (%)	M.p. (°C)	Found (calc.)% C	H	N	M
HA^1	orange	87	90	74.71 (74.67)	6.30 (6.27)	5.84 (5.81)	–
$[Co(A^1)_2].2H_2O$	brown	70	>250	62.58 (62.55)	5.60 (5.56)	4.90 (4.87)	10.32 (10.24)
$[Mn(A^1)_2(AcO)(H_2O)].H_2O$	brown	64	>250	60.94 (60.90)	5.60 (5.55)	4.49 (4.44)	8.78 (8.71)
$[Ru(A^1)_2Cl(H_2O)].2H_2O$	brown	68	157	53.67 (53.64)	5.10 (5.07)	4.21 (4.17)	15.10 (15.06)
HA^2	orange	85	59	74.70 (74.67)	6.23 (6.27)	5.77 (5.81)	
$[Co(A^2)_2].H_2O$	green	71	228	62.60 (62.55)	5.17 (5.21)	4.90 (4.86)	10.31 (10.24)
$[Mn(A^2)_2(AcO)(H_2O)].2H_2O$	black	70	153	59.25 (59.21)	5.28 (5.24)	4.35 (4.32)	8.54 (8.47)
$[Ru(A^2)_2(Cl)(H_2O)]$	brown	65	142	56.64 (56.68)	4.75 (4.72)	4.45 (4.41)	15.97 (15.91)
H_2L^1	orange	80	124	70.25 (70.20)	5.41 (5.36)	7.40 (7.44)	
$[Co_2(L^1)(Cl)_2(H_2O)_2].H_2O$	brown	65	240*	42.74 (42.77)	3.94 (3.89)	4.58 (4.54)	19.16 (19.09)
$[Mn_2(L^1)(AcO)_4(H_2O)_4].H_2O$	brown	66	>250	44.46 (44.43)	4.98 (4.93)	3.49 (3.46)	12.64 (12.57)
$[Ru_2(L^1)(Cl)_4(H_2O)_4].H_2O$	brown	72	>250	33.10 (33.06)	3.47 (3.51)	3.54 (3.51)	25.36 (25.31)
H_2L^2	orange	90	205	73.25 (73.22)	5.24 (5.20)	6.61 (6.57)	
$[Co_2(L^2)(Cl)_2(H_2O)_2].2H_2O$	brown	67	245	45.43 (45.39)	4.40 (4.36)	4.10 (4.07)	17.22 (17.15)
$[Mn_2(L^2)(AcO)_4(H_2O)_4].3H_2O$	black	63	244	45.39 (45.42)	5.30 (4.34)	3.16 (3.12)	12.28 (12.23)
$[Ru_2(L^2)(Cl)_4(H_2O)_4].2H_2O$	black	60	>250	34.69 (34.72)	3.75 (3.78)	3.14 (3.12)	22.55 (22.49)
H_2L^3	brown	85	228	68.34 (68.31)	5.02 (4.98)	6.97 (6.93)	
$[Co_2(L^3)(H_2O)_2(Cl)_2].2H_2O$	brown	65	>250	41.70 (41.66)	3.89 (3.92)	4.26 (4.22)	17.80 (17.77)
$[Mn_2(L^3)(AcO)_4(H_2O)_4].2H_2O$	black	62	>250	43.40 (43.44)	4.76 (4.90)	3.30 (3.27)	12.89 (12.83)
$[Ru_2(L^3)(Cl)_4(H_2O)_4].2H_2O$	brown	60	>250	32.27 (32.30)	3.48 (3.51)	3.24 (3.28)	23.72 (23.65)

*Ω^{-1} cm^2 mol^{-1}.

in the range 576–510 nm Based on the intensities and positions, these bands can be assigned to the *d-d* transitions. However, the spectrum of the complex $[Mn_2(L^3)(AcO)_4(H_2O)_4].2H_2O$ also exhibits the absorption band around 525 nm. In the lower wavenumbers, there are charge transfer (L to M or M to L) transitions. The electronic spectrum of the complex $[Ru(L^1)_2Cl(H_2O)].2H_2O$ in EtOH is shown in Figure 2. In the spectra of the complexes $[Ru(L^1)_2Cl(H_2O)].2H_2O$ and $[Ru_2(L^3)(Cl)_4(H_2O)_4].2H_2O$, the bands at 581 and 550 nm may be assigned to the d-d transitions, respectively. In the other

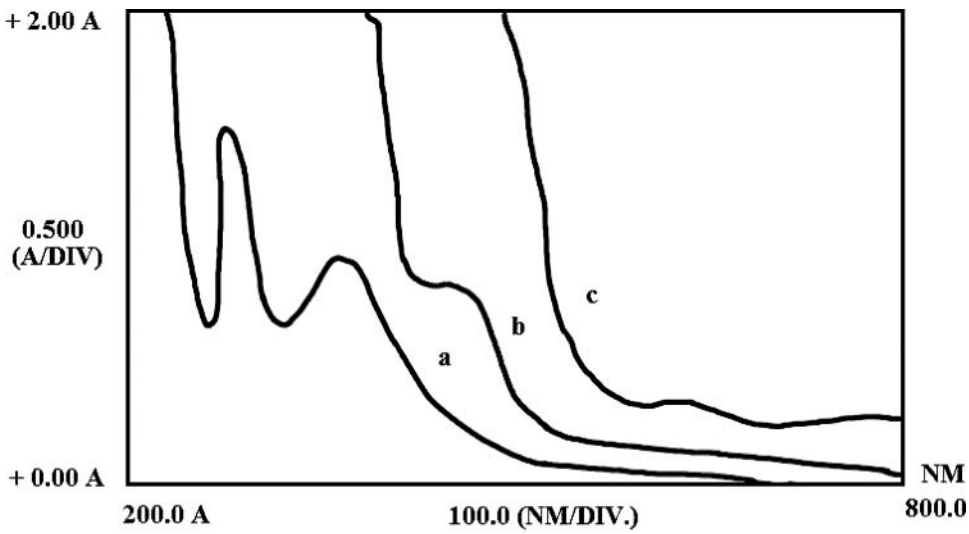

FIG. 2. Electronic spectra of the complexes (a) $[Mn_2(L^3)(AcO)_4(H_2O)_4].2H_2O$, (b) $[Co(A^1)].2H_2O$, and (c) $[Ru(L^1)_2Cl(H_2O)].2H_2O$ using the EtOH solutions (1×10^{-4} M).

Downloaded by [Memorial University of Newfoundland] at 13:47 05 August 2013

Downloaded by [Memorial University of Newfoundland] at 13:47 05 August 2013

TABLE 2
Infrared, electronic, and magnetic moment data of the Schiff base ligands and their metal complexes

Compound	ν(OH)	ν(CH=N)	ν(C-OH)	ν(M-N)	ν(M-O)	λ_{max} (ε_{max}, M^{-1} cm^{-1})	μ_{eff} (B.M.)
HA^1	3420	1602	1365	–	–	449 (2100), 356 (2870), 317 (3015), 280 (4500)	–
$[Co(A^1)].2H_2O$	–	1622	1321	439	530	617 (120), 448 (1057), 356 (1350), 351 (4580), 324 (6700), 278 (9400)	4.40
$[Mn(A^1)_2(AcO)(H_2O)].H_2O$	–	1615	1320	435	528	523 (160), 457 (1040), 356 (2500), 318 (6750), 281 (9900)	4.71
$[Ru(A^1)_2Cl(H_2O)].2H_2O$	–	1622	1321	430	524	581 (134), 452 (1057), 358 (1672), 348 (2305), 306 (5832), 275 (11000)	1.74
HA^2	3408	1612	1369	–	–	452 (1937), 355 (2095), 321 (2871), 305 (3214), 279 (9736)	–
$[Co(A^2)]H_2O$	–	1635	1304	424	582	675 (165), 444 (1867), 346 (3421), 323 (5940), 305 (4590), 275 (7862)	4.55
$[Mn(A^2)_2(AcO)(H_2O)].2H_2O$	–	1602	1309	507	549	567 (200), 460 (965), 454 (2450), 334 (3500), 317 (2300), 280 (8780)	4.75
$[Ru(A^2)_2(Cl)(H_2O)]$	–	1635	1315	480	540	440 (580), 355 (2570), 330 (5700), 305 (6400), 275 (8200)	1.70
H_2L^1	3415	1607	1380	–	–	374 (1890), 346 (3704), 285 (8856)	–
$[Co_2(L^1)(Cl)_2(H_2O)_2]H_2O$	–	1631	1306	502	582	689 (158), 447 (1004), 355 (1877), 346 (2760), 332 (4500), 248 (6780)	4.25
$[Mn_2(L^1)(AcO)_4(H_2O)_4].H_2O$	–	1618	1301	422	538	510 (215), 414 (1400), 357 (2580), 346 (3054), 318 (3580), 276 (8900)	4.82
$[Ru_2(L^1)(Cl)_4(H_2O)_4].H_2O$	–	1645	1255	430	540	425 (1905), 412 (3371), 355 (5238), 334 (7260), 277 (7893)	1.85
H_2L^2	3410	1635	1380	–	–	397 (2387), 365 (4721), 343 (5491), 279 (10084)	–
$[Co_2(L^2)(Cl)_2(H_2O)_2].2H_2O$	–	1616	1367	452	534	731 (105), 377 (3400), 335 (3050), 300 (5200), 275 (9500)	4.7
$[Mn_2(L^2)(AcO)_4(H_2O)_4].3H_2O$	–	1645	1315	442	556	527 (210), 425 (985), 389 (2200), 279 (9805)	4.79
$[Ru_2(L^2)(Cl)_4(H_2O)_4].2H_2O$	–	1606	1252	438	534	415 (1632), 367 (2072), 346 (4367), 275 (6100)	1.80
H_2L^3	3366	1616	1344	–	–	460 (1578), 360 (2458), 349 (3781), 300 (4098), 281 (9045)	–
$[Co_2(L^3)(Cl)_2(H_2O)_2].2H_2O$	–	1631	1307	502	583	651 (270), 457 (1457), 353 (2561), 346 (6800), 275 (7845)	4.68
$[Mn_2(L^3)(AcO)_4(H_2O)_4].2H_2O$	–	1608	1313	422	511	576 (180), 525 (305), 379 (1680), 348 (1720), 310 (4580), 280 (7800)	4.78
$[Ru_2(L^3)(Cl)_4(H_2O)_4].2H_2O$	–	1604	1317	452	543	550 (215), 480 (1305), 369 (1457), 346 (2372), 275 (7600)	1.83

Downloaded by [Memorial University of Newfoundland] at 13:47 05 August 2013

Ru(III) complexes, the d-d bands have not been observed. The lowest energy band is associated with a shoulder near 600 nm. The bands in the range 480–415 nm can be assigned to the the $d_\pi(Ru) \rightarrow \pi^*(L)$ (symmetric) and $d_\pi(Ru^{III}) \rightarrow \pi^*(L)$ (antisymmetric) MLCT (metal-to-ligand charge-transfer) transitions. The next highest energy band near 350 nm may be due to the $d_\pi(Ru) \rightarrow L$ (MLCT) transition. The higher energy bands in the UV region are of intra-ligand p–p* type or charge-transfer transitions involving energy levels that are higher in energy than the ligand lowest unoccupied molecular orbital (LUMO).

The magnetic moment measurements of the complexes have been measured at room temperasture (298 K), and data of the complexes are given in Table 2. The magnetic moments per one manganese ion of the complexes measured at room temperature are in the range 4.71–4.82 μ_B. These values are close to the spin only value of 4.9 μ_B expected for a magnetically diluted high spin d^4 manganese(III) ion. These results indicate that there is little or no intramolecular anti-ferromagnetic coupling between the metal centers of the complexes. In the $[Mn_2(L^m)(AcO)_4(H_2O)_4].xH_2O$ complexes (m: 1, 2 and 3), the two manganese ions are thus separated by the phenylene backbone of the Schiff base ligands making them essentially magnetically isolated.

Tetrahedral and high spin octahedral cobalt(II) complexes each possess three unpaired electrons, but may be distinguished by the magnitude of the deviation of effective magnetic moment value (μeff value) from the spin-only value. Magnetic moments of tetrahedral cobalt(II) complexes with an orbitally degenerate ground term are increased above the spin-only value via contribution from higher orbitally degenerate terms and occur in the range of 4.2–4.7 BM. This is supported by the visible spectra in the range of 675–640 nm assignable to the $^4A_2 \rightarrow {}^4T_1(P)$ transition in a pseudotetrahedral geometry.

The magnetic moment data for the Ru^{III} complexes are in the 1.70–1.85 μ_B range. The magnetic moment values of the Ru^{III} correspond to one unpaired electron suggesting a low spin t_{2g}^5 configuration for the Ru^{III} ion in an octahedral environment.

The H NMR spectra of the ligands were recorded in $(CD_3)_2SO$ solvent using a 300 MHz instrument. The spectra of the ligands H_2L^1-H_2L^3 are shown in Figures 3–5. Spectral data of the ligands are given in Experimental Section. The asymmetric ligands HA^1, HA^2, and H_2L^3 make all the aromatic rings inequivalent. The ligands HA^1, HA^2, and H_2L^3 thus possess 5, 7, and 9 non-equivalent aromatic protons, respectively. Since the electronic environment of many aromatic hydrogen atoms are similar, their signals appear in a narrow chemical shift range. In fact, the aromatic regions of the spectra are complicated due to the overlapping of several signals that have precluded the identification of individual resonances. However, the ligands H_2L^1 and H_2L^2 are symmetric, therefore they possess similar chemical environments. In the spectra of the ligands, the broad bands in the range 10.27–13.21 ppm can be assigned to the hydroxyl proton resonance. The singlet due to the azomethine (–CH=N–) proton in the ligands are in the range δ 8.65–9.12 ppm. As

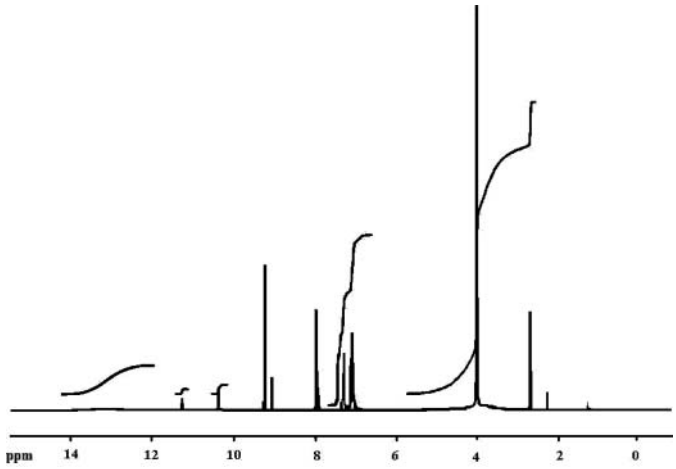

FIG. 3. ^{1}H-NMR spectrum of the ligand H_2L^3.

multiplet, the aromatic ring protons are shown in the range 6.43–8.15 ppm. The very strong singlets in the range 3.75–3.87 ppm are attributed to the protons of the -OCH_3 group. The resonance peak for the COOH proton in the ligand H_2L^3 could be detected around δ 11,17 ppm (broad signal).[18]

Mass spectra of the ligands have been obtained using the LC/MS method. The mass spectra of the ligands HA^1, H_2L^1 and H_2L^3 are shown in Figures 6–8. Spectral data of the ligands are given in the Experimental Section. The mass spectra of the Schiff base ligands indicate high thermal stability. Signals due to the parent ions were observed in all cases. The major peaks in the mass spectrum of the ligands provide an example of the fragmentation patterns observed. The isotopic patterns of the individual signals are in good agreement with those predicted from the isotopic distribution of ligand atoms. In all ligands, the molecular ion peaks are observed as $[M+1]^+$. We investigated all fragmentation products. Among the ligands, we suggest

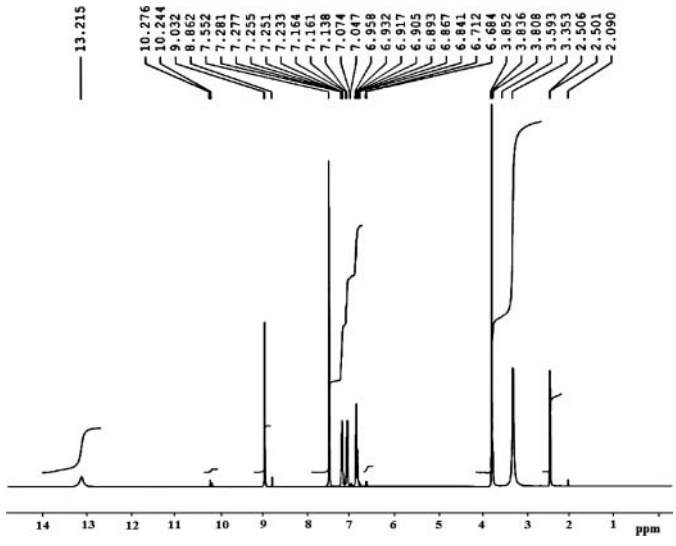

FIG. 4. ^{1}H-NMR spectrum of the ligand H_2L^2.

Downloaded by [Memorial University of Newfoundland] at 13:47 05 August 2013

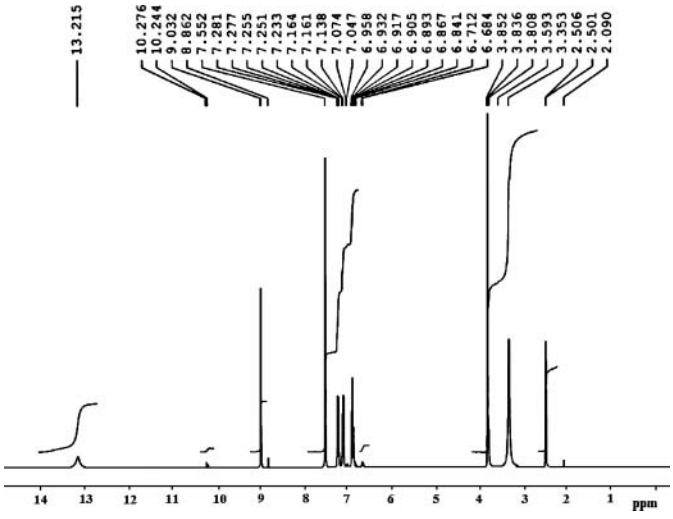

FIG. 5. ^{1}H-NMR spectrum of the ligand H_2L^1.

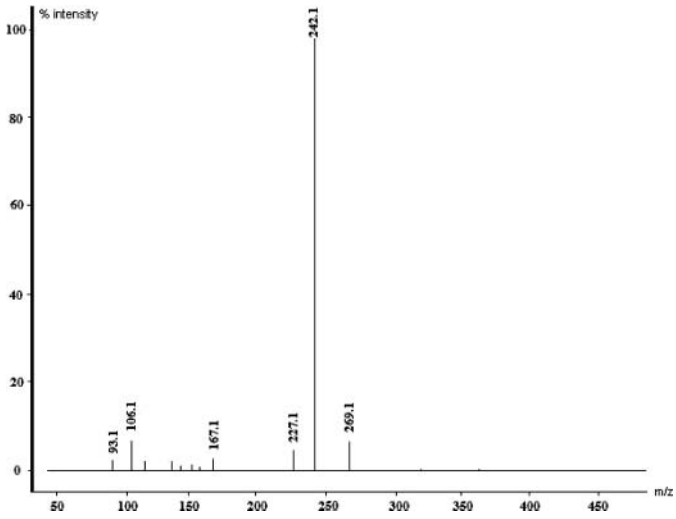

FIG. 7. Mass spectrum of the ligand HA^1.

the fragmentation patterns for the ligands HA^1 and H_2L^3 as in Figure 9.

The thermal stability of the Schiff base complexes Co(II), Mn(III) and Ru(III) have been studied in the range of 298–1273 K. Their thermal decompositions reveal that they contain the adsorbed or coordinated water (chloride or acetate ions) molecules, which are consistent with the elemental and IR spectral analyses (Tables 1 and 2, respectively). The complexes were stable in air at room temperature. They decompose in various ways when heated in air. Considering the temperature (the temperature range 323–373 K) at which the dehydration process of the complexes occur and the way in which it proceeds, it is assumed that the water molecule is in the outer sphere of the complex. For the Co(II) complexes of the ligands HA^1 and HA^2, the anhydrous complex forms CoO in the range of 573–917 K, which is oxidized to Co_3O_4 (919–965 K), the final product of the complex decomposition. The Co(II), Mn(III), and Ru(III) complexes of the ligands H_2L^1-H_2L^3 contain both adsorbed and coordinated water (or Cl^- ion) molecules. After the adsorbed water molecules loss, in the temperature range 383–553 K, the coordinated water molecules AcO^- and Cl^- ions loss from the complexes. When they are heated to higher temperatures, they are decompose directly to the oxides of the corresponding metals (Mn_2O_3, CoO, Ru_2O_3). The dehydration processes are connected with an endothermic effect seen on the DTA curves. The results indicate the following routes thermal decompositions of the complexes:

$$[Mn(L^m)_n(AcO)(H_2O)].xH_2O \rightarrow [Mn(L^m)_n(AcO)(H_2O)] \rightarrow [Mn(L^m)_n] \rightarrow Mn_2O_3$$

$$[Co(L^m)_n].xH_2O \rightarrow [Co(L^m)_n] \rightarrow CoO \rightarrow Co_3O_4$$

$$[Ru(L^m)_n(Cl)(H_2O)].xH_2O \rightarrow [Ru(L^m)_n(Cl)(H_2O)] \rightarrow [Ru(L^m)_n] \rightarrow Ru_2O_3$$

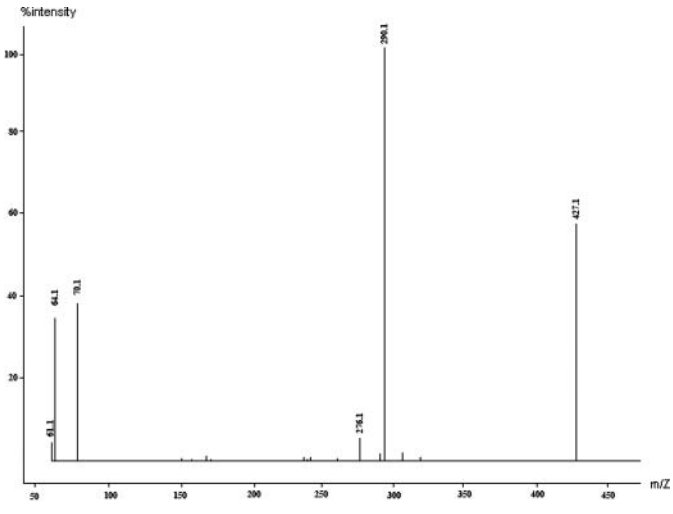

FIG. 6. Mass spectrum of the ligand H_2L^2.

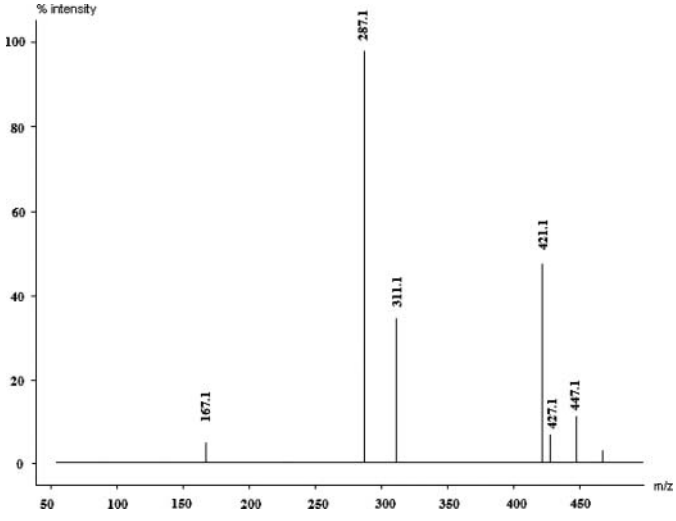

FIG. 8. Mass spectrum of the ligand H_2L^3.

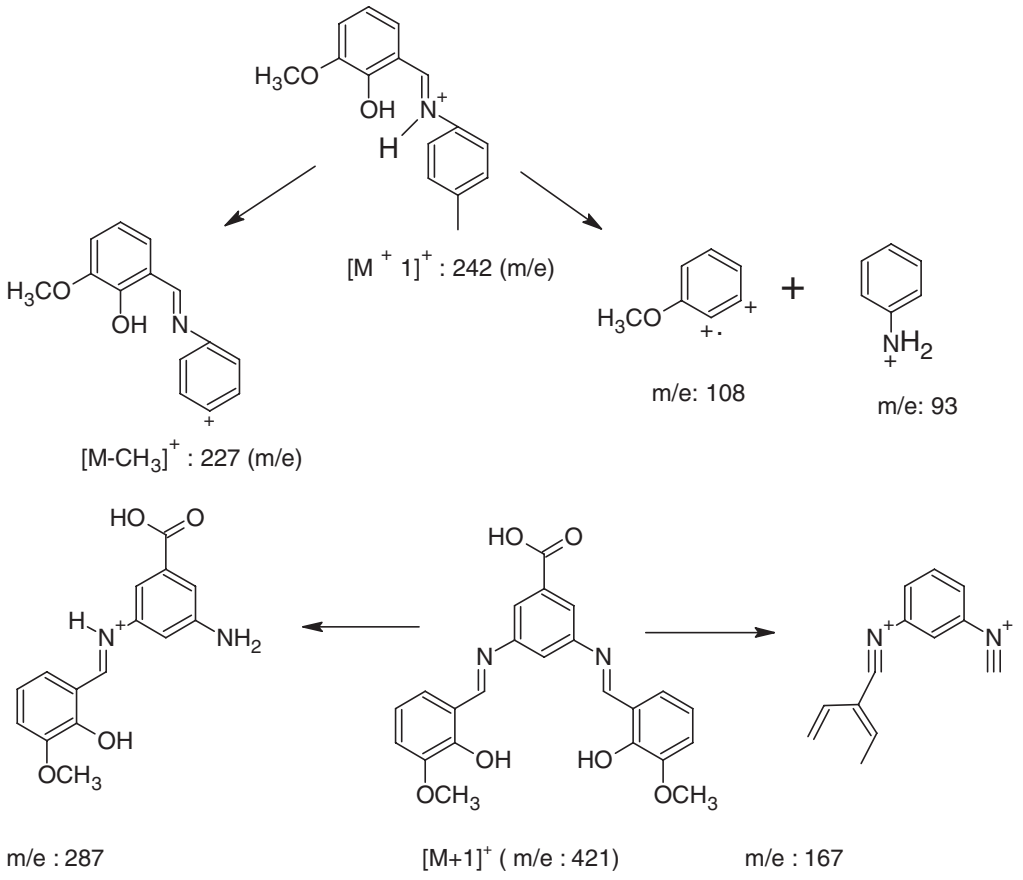

FIG. 9. Fragmentation patterns for the ligands HA^1 and H_2L^3.

In the series of hydrated Mn(III), Co(II), and Ru(III) complexes, the most stable are the complexes of Mn(III) and Co(II), while the least thermally stable is Ru(III) complexes. The thermal stabilities of the anhydrous Co(II), Mn(III), and Ru(III) complexes do not change regularly with increasing atomic number of the element.

All benzylic alcohols used as substrates were known compounds; some of them were of commercial quality (Fluka), while the others were synthesized as described in the literature.[4] Diethyl ether was purified using standard techniques. Bidistilled water was used for preparing the alkaline reagent solutions. The ratio of the substrate and reagent was 1:1. The reactions were performed in alkaline solution at room temperature or at boiling point of the solvent, depending on the substrate used. The reaction was monitored through the change in the color of the reaction mixture from one color to another color. Satisfactory spectroscopic data (IR) were obtained for all products, which were characterized by direct comparison with authentic samples. In a control experiment in which the ligand was omitted, strong peroxide decomposition and no oxidation products were found. In the absence of the manganese salt only substrate and no oxidation products were found. In the case of some primary benzyl alcohols (Table 3), high conversion were obtained. Secondary benzyl alcohols (Table 3) were selectively transformed to the corresponding ketones with satisfactory conversions. In our synthesized ligands, there are several electron-donating substituents. These are OH, OCH_3, and CH_3 groups. These groups are electron-withdrawing with inductive effect, but electron-donating with mesomeric effect. The mesomeric effect had more strength than the inductive effect. However, the ligand H_2L^3 possess the COOH group on the *p*-position. The COOH group is electron-withdrawing from the molecule. The introduction of electron-withdrawing substituents into the aromatic rings increase the yield compared to alcohols with electron-donating substituents. Moreover, substrates with electron-donating substituents, such as 4-(dimethylamino)benzylalcohol, 2-, 3-, 4-methoxybenzylalcohol, 1,2-bis[4-(dimethylamino)phenyl]-2-hydroxyethanone and 2-hydroxy-1,2-bis(4-methoxyphenyl)ethanone (Table 3) reacted less effeciently when compared to substrates containing electron-wirthdrawing groups, such as 2-hydroxy-1,2-diphenylethanone (Table 3). The secondary benzyl alcohols 1,2-bis[4-(dimethylamino)phenyl]-2-hydroxyethanone and 2-hydroxy-1,2-bis(4-

Downloaded by [Memorial University of Newfoundland] at 13:47 05 August 2013

TABLE 3
Catalytic oxidation data of alcohols by the metal complexes

Substrate	Complex	Product	Temp. (°C)	Reaction time (h)	Yield (%)
A	1–3	Aldehyde	b.p.	4–5	30
B	4–6	Aldehyde	b.p.	4	58
C	7–9	Aldehyde	b.p.	3	77
D	10–12	Keton	r.t.	0.5	90
E	13–15	Keton	b.p.	0.5	95
F	1–3	Keton	b.p.	1	100
G	4–6	Keton	r.t.	1	100
H	7–9	Keton	b.p.	0.5	96
I	10–12	Keton	b.p.	1	100
J	13–15	Keton	r.t.	0.5	100
K	1–3	Aldehyde	b.p.	0.5	80

1: $[Co(A^1)].2H_2O$; 2: $[Mn(A^1)_2(AcO)(H_2O)].H_2O$; 3: $[Ru(A^1)_2Cl(H_2O)].2H_2O$;
4: $[Co(A^2)]H_2O$; 5: $[Mn(A^2)_2(AcO)(H_2O)].2H_2O$; 6: $[Ru(A^2)_2(Cl)(H_2O)]$;
7: $[Co_2(L^1)(Cl)_2(H_2O)_2]H_2O$; 8: $[Mn_2(L^1)(AcO)_4(H_2O)_4].H_2O$; 9: $[Ru_2(L^1)(Cl)_4(H_2O)_4].H_2O$; 10: $[Co_2(L^2)(Cl)_2(H_2O)_2].2H_2O$;
11: $[Mn_2(L^2)(AcO)_4(H_2O)_4].3H_2O$;
12: $[Ru_2(L^2)(Cl)_4(H_2O)_4].2H_2O$; 13: $[Co_2(L^3)(Cl)_2(H_2O)_2].2H_2O$;
14: $[Mn_2(L^3)(AcO)_4(H_2O)_4].2H_2O$; 15: $[Ru_2(L^3)(Cl)_4(H_2O)_4].2H_2O$.
r.t.: room temperature, b.p.: boiling point of solvent used. All yields are for pure, isolated products.
A: 2-Methoxy benzyl alcohol, **B**: 3-Methoxy benzyl alcohol, **C**: 4-Methoxy benzyl alcohol; **D**: 2-hydroxy-1,2-diphenylethanone, **E**: 1,2-bis[4-(dimethylamino)phenyl]-2-hydroxyethan-one, **F**: 2-hydroxy-1,2-bis(4-methoxyphenyl)ethanone, **G**: 1,2-bis[4-(dimethylamino)phenyl]-2-hydroxyethanone, **H**: 2-hydroxy-1,2-diphenylethanone, **I**: cyclohexanol, **J**: cyclooctanol,**K**: Cinnamyl alcohol.

Downloaded by [Memorial University of Newfoundland] at 13:47 05 August 2013

methoxyphenyl)ethanone and some primary benzyl alcohols 4-methoxy benzyl-alcohol and [4-(dimethylamino)]benzylalcohol have *p*-substitutents with electron-donating properties with the mesomeric effect, proceed to only low conversions. As the ligand H_2L^3 has the COOH group that electron-withdrawing, according to the other Schiff base complexes, its metal complexes reacted very quickly at room temperature and the reaction went to completion within a few minutes. Other oxidation reactions required a longer reaction time (from half an hour to several hours, Table 3). It appeared that substituents on the aromatic ring affected the yield of benzylic carbonyl product as well as the rate of the reaction. However, a distinct steric effect was observed as ortho substituted substrates react more sluggishly, and in fact 2-methoxybenzyl alcohol was found to be virtually unreactive. High conversions were also obtained when secondary alcohols were oxidized. For example, the oxidation of cyclohexanol and cyclooctanol were found with selectivities up to 99% to the corresponding ketones. For 4-methoxy benzylalcohol, lower selectivities were observed. Perhaps over oxidation to benzoic acid takes place (Figure 10); however, this was not quantified. Other secondary alcohols like 2-hydroxy–1,2-diphenylethanone, 1,2-bis[4-(di-methylamino)phenyl]-2-hydroxyethanone and 2-hydroxy–1,2-bis(4-methoxyphenyl) ethan-one were selectively transformed to the corresponding ketones with high conversions. The ligand HA^2 has the methyl group on the 2-position on the amine ring. The striking influence of the additional methyl groups on the reactivity could be a result of either electronic or steric properties of the ligand. In the oxidation reaction, the order of the activity of the metal complexes is Co > Mn > Ru. Moreover, the binuclear complexes have higher activity than the mononuclear complexes.

Electrochemistry

The redox properties of the ligands were investigated in DMF and DMSO solutions (in nitrogen atmosphere) by cyclic voltammetry and the redox processes are ligand centered only (Table 3). The cyclic voltammograms of the ligands HA^2 and H_2L^3 are seen in Figure 11. For all Schiff-base ligands studied, cyclic voltammograms at a wide range of scan rates from 50 to 500 mVs^{-1} consist of a single cathodic peak at potentials ranging from −0.620 to 1.390 V; no anodic wave, except for the ligand H_2L^3, occurs in the reverse scan. Hence, such a reduction process should correspond to a totally irreversible electron transfer. The ligand H_2L^3 shows two anodic peaks at −1.430 and −0.720 V. These peaks can be attributed to the reduction of the COOH group. This situation indicates that the anodic wave observed corresponds to a two-electron transfer. In fact, the shapes of the anodic waves suggest that they would consist of two overlapped one-electron processes. Such a requirement would arise from the fact that

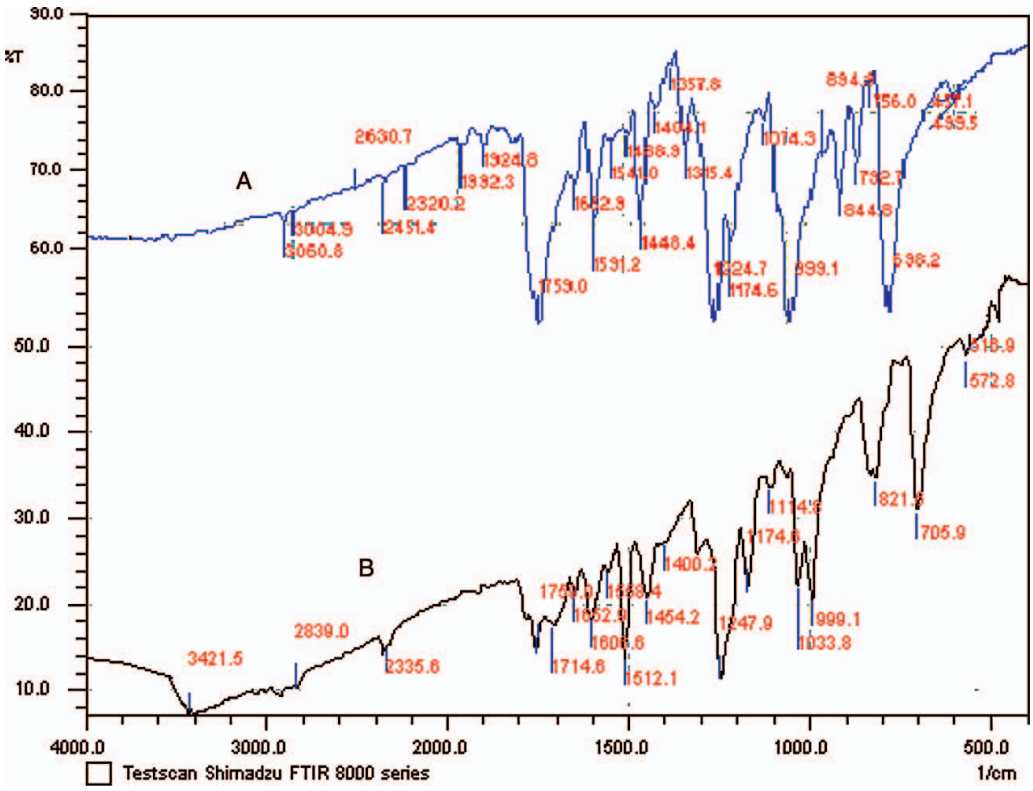

FIG. 10. IR spectra of the (A) 4-methoxy benzaldehyde and (B) 4-methoxy benzoic acid that forms in alcohol oxidation reaction. (Figure is provided in color online.)

both the dielectric constant and the dipole moment of DMF are smaller than those of DMSO. For all Schiff bases under study, this irreversible reduction peak would be ascribed to an intramolecular reductive coupling of the two imine groups to yield a piperazine.[19] Such a process would involve self-protonation reactions where the phenolic hydroxyl groups act as proton donors. On the other hand, in each series of ligands, the cathodic peak potential (*E*pc) corresponding to the intramolecular reductive coupling of the imine groups varies as can be expected from the electronic effects of the substituents at positions 2,2′ and 3,3′. Thus, in the ligands HA^1, HA^2 and H_2L^3, *E*pc becomes more negative according to the sequence OCH_3, CH_3 and COOH, i.e., in order of an increase in both electron-withdrawing and -acceptor qualities of the substituents. This fact agrees with a mechanism involving self-protonation reactions for the electrochemical reduction of the imine groups in the Schiff base ligands in the study.

The redox properties of all the Ru^{III} complexes were investigated in DMF solution (in nitrogen atmosphere) by cyclic voltammetry and the redox processes are metal centered only (Table 3). The number of electrons transferred in the electrode reaction for a reversible couple can be determined from the separation between the peak potential.

$$\Delta Ep = Epa - Epc = \frac{0.0591}{n}$$

where E_{pa}, E_{pc}, and n are anodic potential, cathodic potential and the number of electrons transferred, respectively. Thus, a one electron process exhibits a ΔEp approximately 0.059V. At slower scan rate, the peak separation for the cathodic and anodic cyclic voltammetric peak potentials is very close to 60–70 mV, indicating that the number of electrons transferred should be 1.0. Cyclic voltammograms of all the complexes (1×10^{-3} M) exhibit a reversible oxidation and reversible reduction peaks at the scan rates 50, 100, and 500 mVs^{-1}. A representative cyclic votammograms of $[Ru_2(L^1)(Cl)_4(H_2O)_4].H_2O$ (C) and $[Ru(A^1)_2Cl(H_2O)].2H_2O$ (D) are shown in Figure 12. In the scan rate 50 mvs^{-1}, all the Ru(III) complexes showed well-defined waves in the range ($E_{1/2}$)+1.235 to +0.130 V (Ru^{IV}/Ru^{III}) and −1.650 to −0.015 V (Ru^{III}/Ru^{II}) *versus* Ag/AgCl, ut this property changes in the scan rate 500 mVs^{-1}. For scan rate 500 mVs^{-1}, the ratio *i*p/SR (*i*p = peak current; sr = scan rate) was approximately one, the peak separation being independent of the scan rate. This indicates that the electron transfer is reversible and the mass transfer is limited. It has been observed that the complexes show quasi-reversible redox processes, which did change with change in scan rates. The electron donating group (-OH) as the mesomeric effect ability of the substituent on the phenyl ring of the Schiff base favors oxidation of Ru^{III} to Ru^{IV}.[20] The electrochemistry of these complexes in DMF consists of a well-defined Ru(III/II) oxidation couple, the position of which is highly dependent upon the substituent (see Table 4).

Downloaded by [Memorial University of Newfoundland] at 13:47 05 August 2013

Downloaded by [Memorial University of Newfoundland] at 13:47 05 August 2013

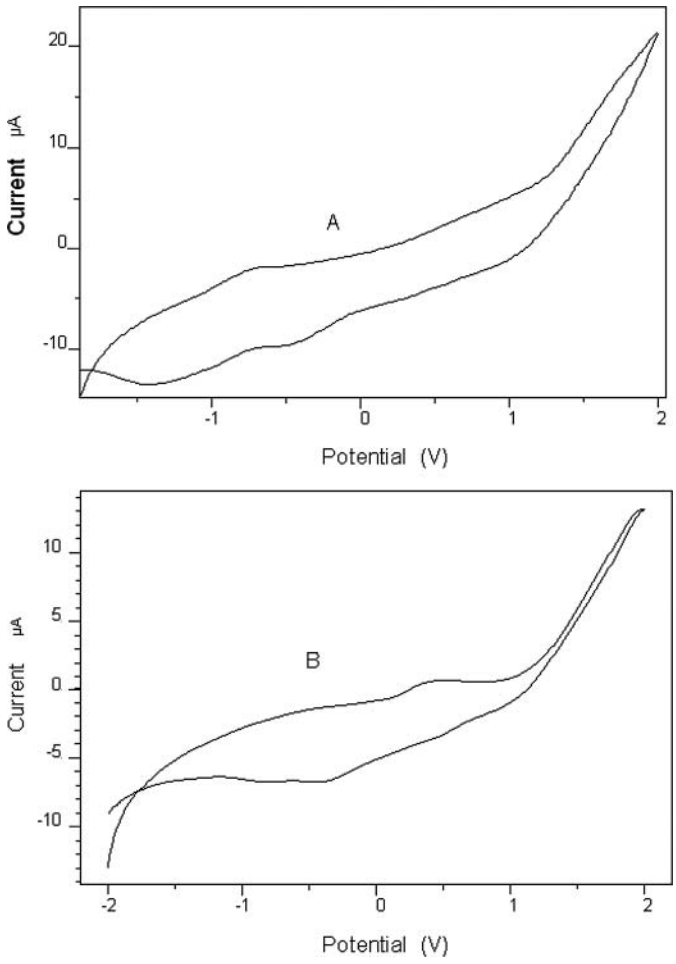

FIG. 11. Cyclic voltammetry curves of the ligands (A) H_2L^3 and (B) HA^2 in DMF in the presence of tetrabutylammonium tetrafluoroborat (0.1 M) (scan rate: 500 mv/s).

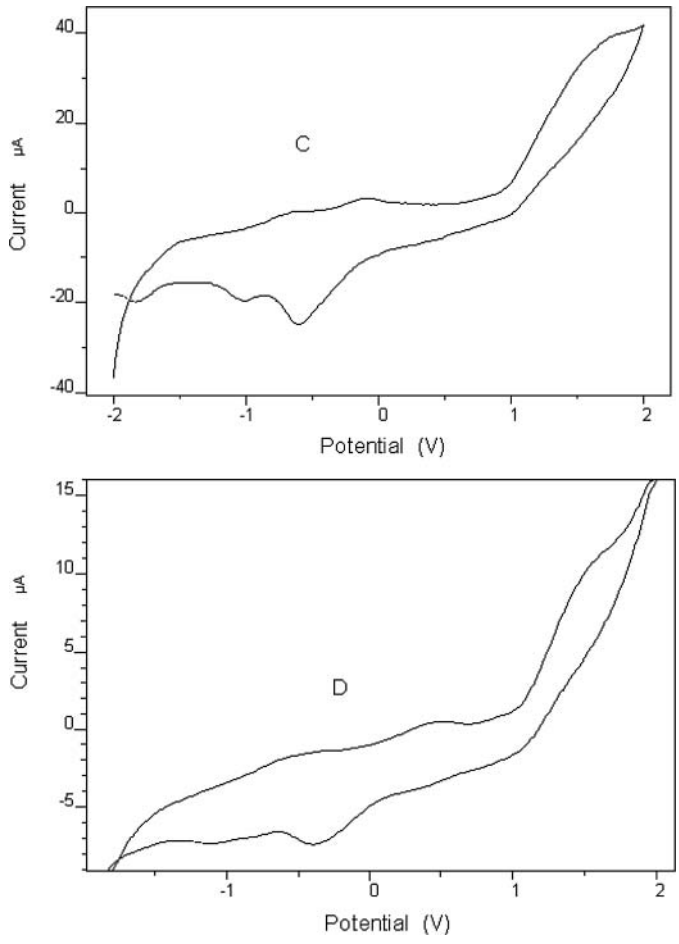

FIG. 12. Cyclic voltammetry of (C) $[Ru_2(L^1)(Cl)_4(H_2O)_4].H_2O$ and (D) $[Ru(A^1)_2Cl(H_2O)].2H_2O$ in DMF in the presence of tetrabutylammonium tetrafluoroborat (0.1 M) (scan rate: 100 mv/s).

In DMF, the $E_{1/2}$ data are the 570, 535, 1235, 80, and −1650 mV for the CH_3 and OCH_3 (for HA^1 and HA^2), dimethoxy (for H_2L^1 and H_2L^2), and dimethoxy and carboxy (for H_2L^3) groups, respectively. The shifts in oxidation potential are a reflection of the donor-acceptor ability of the substituents, with the electron-donating methoxy substituent shifting the Ru(III/II) oxidation to more positive potentials, and the electron-withdrawing carboxy substituent shifting the Ru(III/II) couple to less positive potentials.

$$[Ru^{III}(X)Cl(H_2O)] \leftrightarrow [Ru^{IV}Cl(H_2O)(X)]^+ + e^-$$

The redox properties of the Co^{II} complexes were investigated in DMF solution by cyclic voltammetry, and the redox processes are metal centered only (Table 3). Cyclic voltammogram of all the complexes (1×10^{-3} M) exhibit a reversible oxidation and reversible reduction peaks at the scan rate 100 mVs^{-1}. In the mononuclear Co(II) complexes, it is shown that a reversible oxidation (1.510 and 1.730 V) and reversible reduction peaks at the scan rate 100 mVs^{-1}. A representative cyclic votammograms of $[Co_2(L^3)(Cl)_2(H_2O)_2].2H_2O$ (E) and $[Co(L^1)].2H_2O$ (F) are shown in Figure 13. In the mononuclear Co(II) complexes, it is shown that a reversible oxidation (1.510 and 1.730 V) and reversible reduction (−1.880 and 0.370 V) peaks at the scan rate 50 mVs^{-1}. These peaks change to 0.420 and 0.190 V for oxidation, and −1.840 and −0.640 V for reduction processes, respectively. One quasi-reversible redox couple is a common feature of the cyclic voltammograms of the Co(II) complexes. The values of ΔEp and peak current ratios of the waves are consistent with one-electron transfer processes. The reduction wave approximately at 0.8 V is assigned to the $Co^{II/I}$ couple.

$$[Co^{II}(A^{1-2})] \cdot H_2O + e^- \rightarrow [Co^{I}(A^{1-2})]H_2O$$

In the binuclear Co(II) complexes, there are two reduction and oxidation peaks. These peaks are revesible. For the scan rate 50 mVs^{-1}, the anodic and cathodic peaks are in the range −1.30 to 0.36 V and −1.00 to 1.91 V. When the scan rate is increased, these peaks change. An unsaturated nitrogen as the

Downloaded by [Memorial University of Newfoundland] at 13:47 05 August 2013

TABLE 4
Electrochemical data of Schiff base complexes

Compounds	*E_{pa} (V)	*E_{pc} (V)	$E_{1/2}$ (mV)	ΔE_p (mV)	**E_{pa} (V)	**E_{pc} (V)	$E_{1/2}$ (mV)	ΔE_p(mV)
HA^1	–	1.39	695	−1390	–	–	–	–
$[Co(A^1)].2H_2O$	−1.88	1.51	185	−3390	−1.84	0.42	−710	−2260
$[Mn(A^1)_2(AcO)(H_2O)].H_2O$	−0.09, 0.71	0.19, 1.05	880, 450	−280	−0.15	0.60, 1.20	−225, 525	−1235
$[Ru(A^1)_2Cl(H_2O)].2H_2O$	−1.88, −0.39	1.46	−210, 535	−3340	−0.99, −0.59	−0.52, −0.10	−470, −245	−1510
HA^2	–	-0.620	-310	620	–	–		
$[Co(A^2)]H_2O$	0.370	1.730	1050	−1360	−0.64	1.51	870	−1075
$[Mn(A^2)_2(AcO)(H_2O)].2H_2O$	−0.20, 0.82	1.30, 0.87	550, 845	−1500	−0.42	1.25, 0.88	415, 230	−1670
$[Ru(A^2)_2(Cl)(H_2O)]$	−0.25, 0.32	1.39, −0.07	570, 130	−1640	−0.42, 0.77	−0.53, 1.48	−55, 1125	110
H_2L^1	–	0.46	230	−460	–	–		
$[Co_2(L^1)(Cl)_2(H_2O)_2]H_2O$	−1.10, 0.36	0.47, 0.21	−315, 285	−1570	−1.50, −0.52	0.68	−410, 80	−820
$[Mn_2(L^1)(AcO)_4(H_2O)_4].H_2O$	−0.32	−0.16	−240	−160	−1.52	0.06	−730	−1580
$[Ru_2(L^1)(Cl)_4(H_2O)_4].H_2O$	−1.88, 0.35	−0.59, −0.38	1235, −15	−1290	−0.66	−0.44	−550	−220
H_2L^2	–	1.12	560	−1120	–	–		
$[Co_2(L^2)(Cl)_2(H_2O)_2].2H_2O$	−0.24, 0.25	1.91, 0.08	835, 165	−2150	−0.56	1.25, 0.75	345, 95	−1810
$[Mn_2(L^2)(AcO)_4(H_2O)_4].3H_2O$	−0.96	0.69	135	−1650	−0.76	1.22	230	−1980
$[Ru_2(L^2)(Cl)_4(H_2O)_4].2H_2O$	−1.10, −0.37	1.37, 0.41	80, 35	−2470	−1.26, −0.53	−0.55, 0.48	−905, −25	−710
H_2L^3	−1.43, −0.72	−0.62	1025, 670	−810	–	–		
$[Co_2(L^3)(Cl)_2(H_2O)_2].2H_2O$	−1.30, 0.30	1.66, −1.00	180, −350	−1960	0.89, −0.60	1.15, 0.42	1020, −90	−260
$[Mn_2(L^3)(AcO)_4(H_2O)_4].2H_2O$	0.30, −0.36	1.01, −0.11	650, −235	−710	−1.30, −0.91	0.10	−600, −405	−1200
$[Ru_2(L^3)(Cl)_4(H_2O)_4].2H_2O$	−1.88, −0.22	−1.42, −0.74	−1650, −480	−460	−0.41	−0.49	−450	80

*scan rate: 50 mV/s, ** scan rate: 500 mV/s. Supporting electrolyte: tetrabutylammonium tetrafluoroborat (0.1 M); concentration of the complex: 10^{-3} M. All the potentials are referenced to Ag/AgCl; where E_{pa} and E_{pc} are anodic and cathodic potentials, respectively. $E_{1/2} = 0.5 \times (E_{pa} + E_{pc})$, $\Delta Ep = E_{pa} - E_{pc}$.

Downloaded by [Memorial University of Newfoundland] at 13:47 05 August 2013

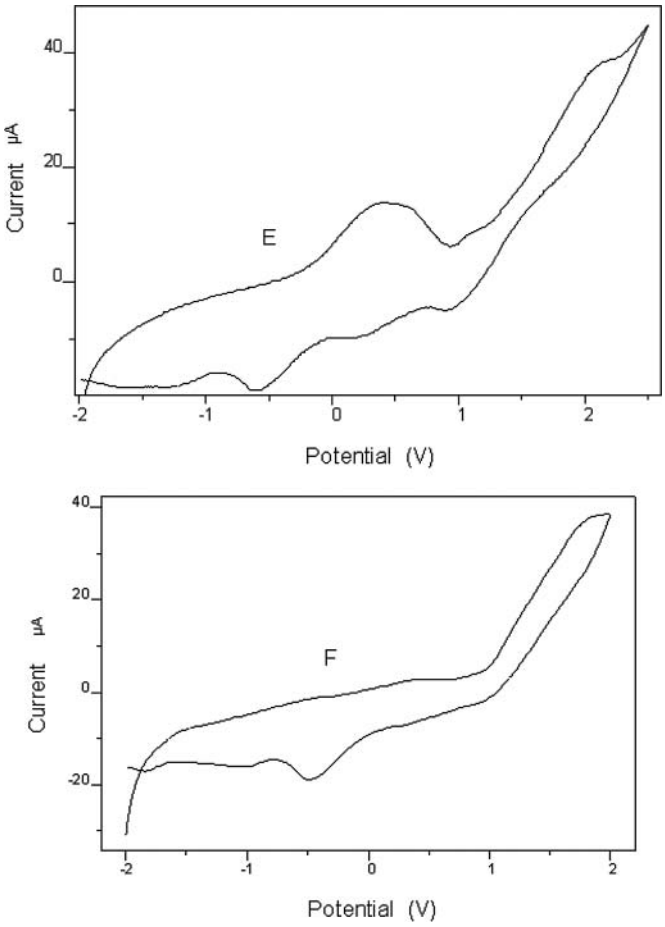

FIG. 13. Cyclic voltammetry curves of $[Co_2(L^3)(Cl)_2(H_2O)_2].2H_2O$ (E) and $[Co(L^1)].2H_2O$ (F) in DMF in the presence of tetrabutylammonium tetrafluoroborat (0.1 M) (scan rate: 500 mv/s).

donor atom in the ligand stabilizes a more low oxidation state, such as Co^I, than a saturated one, by π-back bonding between the metal and the nitrogen atoms.

Cyclic voltammograms of the M(III) complexes were measured in DMF and DMSO over the potential range from + 2.0 to −2.0 V (Ag/AgCl). Quasi reversible redox waves were observed in the range 1.30 to −0.11 V and 1.215 to −1.520 V for the Mn(III) complexes in the different scanning rates (Table 4). By the introduction of an electron-withdrawing substituent, COOH group, the redox potentials of of the complexes of the ligands H_2L^3 are shifted to more positive values than those of other complexes. These shifts can be explained in terms of a decrease in the electron density on the central manganese ion in the complexes. Both of the reduction and oxidation at these potentials are found to be two electron processes. This means that the reduction and oxidation processes of these mono and binuclear complexes may undergo two electron transfer processes.

REFERENCES

1. Pecoraro, V.L. In: *Manganese Redox Enzymes*, Pecoraro V.L.(ED.), VCH: New York, **1992**, 197–232.
2. Doble, D.M.J.; Benison, C.H.; Blake, A.J.; Fenske, D.; Jackson, M.S.; Kay, R.D.; Li, W.S. Template assembly of metal aggregates by iminocarboxylate ligands. *Angew Chem. Schro. der, Int. Ed. Engl*. **1999**, *38*, 1915–1918
3. (a) DuBois, J.; Hong, J., Carreira, E.M.; Day, M.W. Nitrogen transfer from a nitridomanganese(V) complex: Amination of silyl enol ethers. *J. Am. Chem. Soc*. **1996**, *118*, 915–916. (b) Finney, N.S.; Pospisil, P.J.; Jacobsen, E.N. On the viability of oxametallacyclic intermediates in the (salen)Mn-catalyzed asymmetric epoxidation. *Angew. Chem. Int. Ed. Engl*. **1997**, *36*, 1720–1723.
4. Larock, R.C. *Comprehensive Organic Transformations*; VCH Publishers: New York, **1989**, pp. 604–615.
5. Krohn, K.; Vinke, I.; Adam, H. Transition-metal catalyzed oxidations. Zirconium-catalyzed oxidation of primary and secondary alcohols with hydroperoxides. *J. Org. Chem*. **1996**, *61*, 1467–1472.
6. Inokuchi, T., Nakagawa, K., Torii, S. One-pot conversion of primary alcohols to alpha-oxygenated alkanals with tempo in combination with molecular-oxygen and ruthenium complex. *Tetrahedron Lett*. **1995**, *36*, 3223–3226.
7. Balsells, J., Mejorado, L., Phillips, M., Ortega, F., Aguirre, G., Somanathan, R., Walsh, P.J. Synthesis of chiral sulfonamide/Schiff base ligands. *Tetrahedron Asymm*. **1998**, *9*, 4135–4142.
8. Sima, J. Mechanism of photoredox reactions of iron(III) complexes containing salen-type ligands. *Crao. Chem. Acta* **2001**, *74*, 593–600.
9. Ouyang, X.M.; Fei, B.L.; Okamuro, T.A.; Sun, W.Y.; Tang, W.X.; Ueyama, N. Synthesis, crystal structure and superoxide dismutase (SOD) activity of novel seven-coordinated manganese(II) complex with multidentate di-Schiff base ligands. *Chem. Lett*. **2002**, *3*, 362–363.
10. Raman, N.; Raja, Y.P.; Kulandaismy, A. Synthesis and characterisation of Cu(II), Ni(II), Mn(II), Zn(II) and VO(II) Schiff base complexes derived from o-phenylenediamine and acetoacetanilide. *Proc. Ind. Acad. Sci. (Chem. Sc.)* **2001**, *113*, 183–189.
11. Datta, A.; Karan, N.K.; Mitra, S.; Rosair, G. Synthesis and structural characterization of $[Cu(NH_2CH_2C_6H_4N{=}CHC_5H_5N)Cl\text{-}2]$. *Z. Naturf*. **2002**, *57*, 999–1002.
12. Gao, W.T.; Zheng, Z. Synthetic studies on optically active Schiff-base ligands derived from condensation of 2-hydroxyacetophenone and chiral diamines. *Molecules* **2002**, *7*, 511–516.
13. El-Sonbati, A.Z.; El-Bindary, A.A. Stereochemistry of new nitrogen containing aldehydes. V. Novel synthesis and spectroscopic studies of some quinoline Schiff bases complexes. *Polish J. Chem*. **2000**, *74*, 621–630.
14. Vogel, A.I. *Test Book of Practical Organic Chemistry*, 5th ed.; Longman: London, **1989**.
15. Nakamoto, K. *Infrared Spectra of Inorganic and Coordination Compounds*, 2nd Edn; Wiley Inter-Science: New York, **1963**, pp. 108253.
16. Dey, K.; Bhowmik, R.; Sarkar, S. Coordination behaviour of 2-(1-carboxyl-2-hydroxyphenyl)benzothiazoline. *Synth. React. Inorg. Met-Org. Chem*. **2002**, *32*, 1393–1408.
17. Isse, A.A.; Gennaro, A.; Vianello, E. Electrochemical reduction of Schiff base ligands H(2)salen and H(2)salophen. *Electrochim. Acta* **1997**, *42*, 2065–2071.
18. El-Shahawi, M.S.; Shoair, A.F. Synthesis, spectroscopic characterization, redox properties and catalytic activity of some ruthenium(II) complexes containing aromatic aldehyde and triphenylphosphine or triphenylarsine. *Spectrochim. Acta Part:A* **2004**, *60*, 121–127.